An Evaluation of Different Constitutive Models to Predict the Directional Response of a Reconstituted Fine-Grained Soil

C. Tamagnini*, D. Mašin†, D. Costanzo#, and G. Viggiani¶

*Università degli Studi di Perugia, Italy
tamag@unipg.it
†Charles University, Prague, Czech Republic
#Politecnico di Torino, Italy
¶Laboratoire 3S, UJF/INPG/CNRS, Grenoble, France

1 Introduction

The directional character of the mechanical response of fine-grained soils, i.e., its dependence on the loading direction, has been the subject of several studies throughout the last decades, including both experimental and theoretical investigations. On the experimental side, some pioneering contributions were provided in the early seventies, see e.g., [17, 37]. Notable examples of more recent contributions can be found in [2, 3, 11, 28].

On the theoretical side, a major improvement of classical plasticity as applied to clays has been provided by the introduction of the so-called nested-surface kinematic hardening theories of plasticity, originating from the works of Prevost [24], Mroz et al. [21], and Hashiguchi [14]. These latter studies were essentially motivated by the need of improving available design approaches for those practical applications where soil is subject to cyclic loading conditions, e.g., earthquake and offshore engineering. Later studies on shear banding in soils as a bifurcation problem [25,27] showed the need to take into account the *incrementally nonlinear* character of the material response – i.e., a dependence of soil tangent stiffness on the strain rate direction, see, e.g., [8, 32] – and motivated the development of a class of constitutive theories which depart from the framework of plasticity and rather can be seen as a generalization of Truesdell theory of hypoelasticity [34]. A distinctive feature of this approach is the absence of any kinematic decomposition of strain rates into reversible and irreversible parts. An important example in this respect is provided by the theory of hypoplasticity, as defined by Kolymbas [15], see also [16].

More generally, it turns out that a proper description of soil behavior as a function of loading direction not only is useful for modeling the response of geotechnical structures to cyclic loading or for analyzing localization phenomena, but it is also a key ingredient in the analysis of any geotechnical structure

where different zones of soil experience widely different stress-paths, both in size and direction, e.g., deep excavations and tunnels. This has been demonstrated in a number of practical applications, e.g., [10, 29, 35, 36].

The objective of this work is to assess the performance of some advanced constitutive models in reproducing the incremental behavior of a soft, normally consolidated clay as observed in laboratory tests performed along a number of different stress-paths, all originating from a common initial state (*stress-probes*). Two particular classes of inelastic models have been selected for the comparison. On the one hand, the three-surface kinematic hardening model proposed in [30, 31] has been chosen as a representative of advanced soil plasticity approaches. On the other hand, three different versions of hypoplasticity have been considered: the CLoE model [5]; the clay K–hypoplastic model recently proposed by [18], and an enhanced version of this last model, embedding the concept of intergranular strain [23] as an additional internal state variable. Finally, the classical modified Cam-Clay model [26] has been also considered for reference. The results obtained from a large program of stress-probing tests on a soft normally consolidated clay [7] are used herein both for the calibration of the five models, and as a benchmark for the evaluation of the models performance.

The details of the experimental program and a complete account of the experimental results are given in [7], and will be only briefly recalled herein. The results obtained from standard isotropic or triaxial compression and extension tests, starting from an isotropic state, have been used for the calibration of the models. The assessment of models performance has been carried out with reference to a different set of data, obtained from axisymmetric stress-probing tests starting from an anisotropic initial stress state. Predicted and observed directional responses are compared in terms of incremental response envelopes, as defined in [33], which provides a global picture of the models performance over a wide range of loading directions.[1]

2 Experimental Program

The material tested (Beaucaire Marl) is a low plasticity silty clay coming from southern France. The tests were performed on reconstituted material, prepared by thoroughly mixing known quantities of natural soil with distilled water, to a water content approximately equal to 1.5 times the liquid limit. The slurry was then consolidated in a large consolidometer up to a nominal vertical effective stress of 75 kPa. Full details of the experimental procedures employed in the testing program are given in [7].

All tests were carried out using a Bishop and Wesley-type triaxial cell, with fully automated feedback-control. Standard soil specimens, 38.1 mm in diameter and 76.2 mm high, were used in all the tests. Axial load was

[1] In the following, the usual sign convention of soil mechanics (compression positive) is adopted throughout. In line with Terzaghi's principle of effective stress, all stresses are *effective* stresses.

measured by means of an internal load cell. Cell and pore water pressures were measured by means of pressure transducers. Assessments of system scatter showed that stresses could be resolved and controlled to within 0.5 kPa. Axial displacements were measured by means of an external LVDT, with a 10 mm range, and an external proximity transducer having a 2 mm range. Internal and external strain measurements were found to be equivalent to all practical purposes, and reliable down to a minimum axial strain of 0.05%. Volume changes were measured by means of an Imperial College-type volume gauge, with a 50 mm^3 range and a resolution of 0.035% in terms of volume strain. The overall accuracy of volume strain measurements, also depending on possible temperature effects and the stiffness of drainage lines, was evaluated to be approximately 0.05%. This figure also applies to radial strains, which were not directly measured, but rather computed from axial and volume strains.

The testing program consisted of 20 drained stress probes (including two backup tests), starting from a common initial stress state and pointing in different directions in the triaxial plane. Two different initial stress states were considered: the first one (state A) is located on the isotropic axis at mean stress $p = 150$ kPa; the second one (state B) is characterized by the same value of p and a deviator stress $q = 60$ kPa. Both states A and B were reached upon stress-controlled consolidation along a constant q/p path ($q/p = 0$ for state A, $q/p = 0.4$ for state B). Each stress probe from an initial state $(\sigma_{a0}, \sigma_{r0})$ is described by the following parametric equations:

$$\Delta\sigma_a := \sigma_a - \sigma_{a0} = R_\sigma \sin\alpha_\sigma \tag{1}$$

$$\sqrt{2}\,\Delta\sigma_r := \sqrt{2}\,\sigma_r - \sigma_{r0} = R_\sigma \cos\alpha_\sigma, \tag{2}$$

where $R_\sigma = \|\Delta\boldsymbol{\sigma}\|$ denotes the norm of the stress increment, and α_σ represents its direction in the Rendulic plane of stress increments ($\Delta\sigma_a : \sqrt{2}\,\Delta\sigma_r$, see Fig. 1a). Each stress probe was continued up to a R_σ value corresponding either to a "failure" state, or to a prescribed maximum value of the cell pressure.

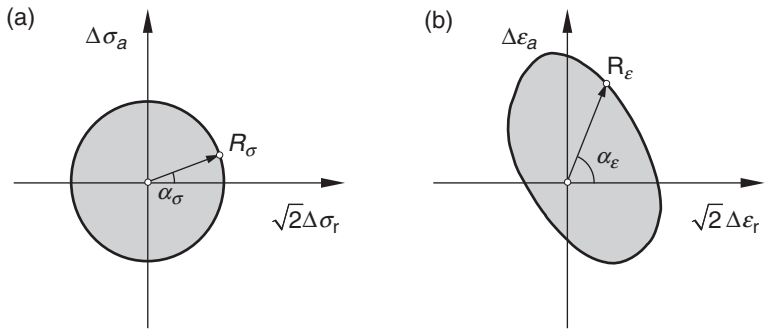

Fig. 1. Response envelope concept: (**a**) input stress probes; (**b**) output strain envelope

Table 1. Details of the experimental stress-probing program, after [7]

test #	initial state	α_σ (deg.)	α_σ^{pq} (deg.)	test #	initial state	α_σ (deg.)	α_σ^{pq} (deg.)
Tx124	A	0	303.69	Tx118	B	0	303.69
Tx128	A	35	0.00	Tx115	B	35	0.00
—	—	—	—	Tx130	B	46	21.91
Tx121	A	90	71.57	Tx132	B	90	71.57
Tx126	A	126	90.00	Tx119	B	126	90.00
—	—	—	—	Tx116	B	154	104.49
Tx123	A	180	123.69	—	—	—	—
Tx127	A	215	180.00	Tx134	B	215	180.00
—	—	—	—	Tx129	B	226	201.91
Tx122	A	270	251.57	Tx117	B	270	251.57
Tx125	A	305	270.00	Tx113	B	305	270.00

All probes were carried out under stress control, applying a constant rate of the stress increment norm approximately equal to $2.5\,\mathrm{kPa\,h^{-1}}$. Note that for each initial state, the testing program included as particular cases convnetional triaxial, constant p and isotropic, compression and extension paths. The loading directions α_σ prescribed for each probe are listed in Table 1. The stress probe direction in the $q:p$ plane, α_σ^{pq}, calculated from the stress invariant increments Δp and Δq as:

$$\Delta p = \frac{1}{3}\left(\Delta\sigma_a + 2\Delta\sigma_r\right); \quad \Delta q = \Delta\sigma_a - \Delta\sigma_r \tag{3}$$

$$\sin\alpha_\sigma^{pq} = \frac{\Delta q}{\sqrt{(\Delta p)^2 + (\Delta q)^2}}; \quad \cos\alpha_\sigma^{pq} = \frac{\Delta p}{\sqrt{(\Delta p)^2 + (\Delta q)^2}} \tag{4}$$

is also reported in the same table. A picture of the stress paths originating from the initial state B in the q:p plane is shown in Fig. 2.

3 Constitutive Models Considered

3.1 3-SKH Model

The 3-SKH model is an advanced example of the kinematic hardening plasticity models for soils. It can be considered an evolution of the classical modified Cam-Clay model [26] and the two-surface kinematic hardening model proposed in [1]. The main feature of the model consists in the introduction of an additional kinematic *history surface* – as defined in [30], see Fig. 3 – motivated by experimental findings about the influence of the recent stress history on soil behavior [2]. The general formulation of the 3-SKH model is given in [31].

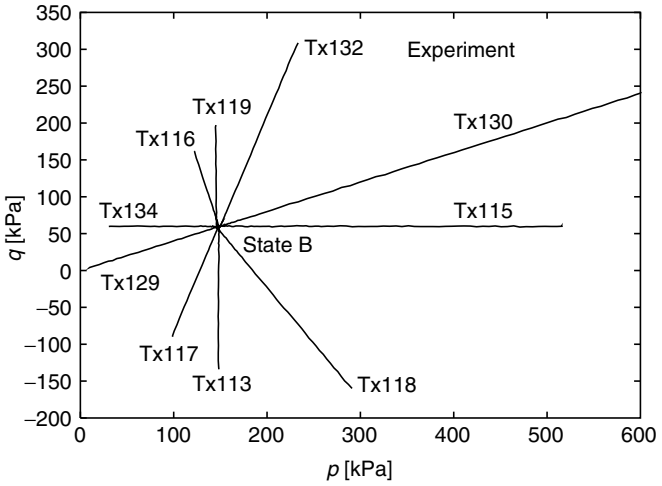

Fig. 2. Experimental stress paths from state B

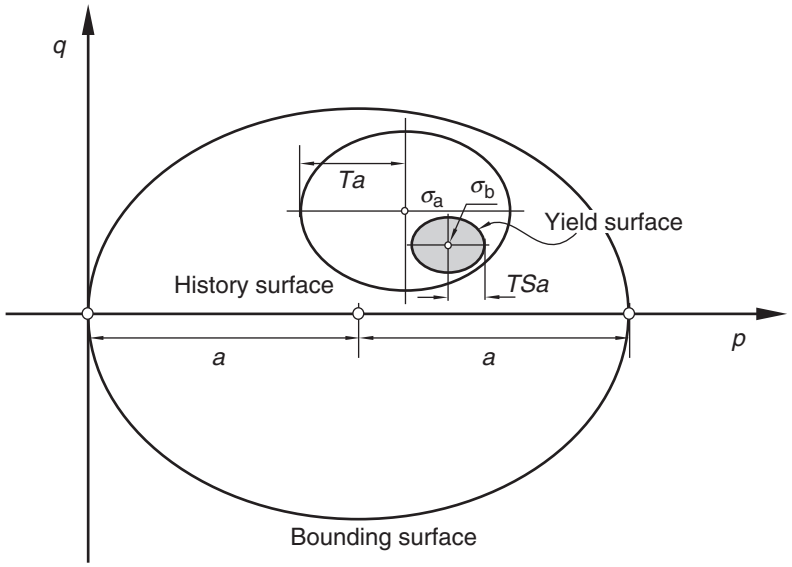

Fig. 3. Sketch of the characteristic surfaces of the 3-SKH model

3.2 CLoE Hypoplastic Model

The hypoplastic model CLoE originates from the pioneering work of Chambon and Desrues on strain localization in incrementally nonlinear materials [4, 9]. The constitutive equation is given, in rate-form, by:

$$\dot{\boldsymbol{\sigma}} = \boldsymbol{\mathcal{A}}(\boldsymbol{\sigma})\dot{\boldsymbol{\epsilon}} + \boldsymbol{b}(\boldsymbol{\sigma})\,\|\dot{\boldsymbol{\epsilon}}\|\,. \tag{5}$$

The first term on the right-hand side yields an incrementally linear response, while the second accounts for incremental nonlinearity via a linear dependence on the norm of the strain rate tensor. To keep the formulation as simple as possible, the set of state variables is limited to the stress tensor $\boldsymbol{\sigma}$.

The two constitutive tensors $\boldsymbol{\mathcal{A}}$ and $\boldsymbol{b}$ appearing in (5) are homogeneous functions of degree one of the stress tensor, for which no explicit expression is assumed. Rather, $\boldsymbol{\mathcal{A}}$ and $\boldsymbol{b}$ are obtained via an interpolation procedure based on the assigned material responses at some suitably defined image points, located along special loading paths (*basic paths*). These are selected among those stress-paths that are experimentally accessible by means of conventional laboratory tests. Details on the mathematical formulation of the material response for the basic paths and on the interpolation procedure are given in [5].

3.3 K–Hypoplastic Models for Clays

The basic formulation of K–hypoplasticity for rate-independent fine-grained soils has been recently developed in [18]. The model combines the mathematical structure of K–hypoplastic models for granular soils – see e.g., [38] and references therein – with key concepts of critical state soil mechanics through the notion of generalised hypoplasticity [22]. The constitutive equation is given, in rate-form, by:

$$\dot{\boldsymbol{\sigma}} = f_s \boldsymbol{\mathcal{L}} : \dot{\boldsymbol{\epsilon}} + f_s f_d \boldsymbol{N}\,\|\dot{\boldsymbol{\epsilon}}\|\,. \tag{6}$$

Explicit, closed-form expressions for the two tensors $\boldsymbol{\mathcal{L}}(\boldsymbol{\sigma})$ and $\boldsymbol{N}(\boldsymbol{\sigma})$ and for the scalar functions $f_s(p)$ and $f_d(p, e)$ are provided in [18]. It must be noted that, although (5) and (6) appear quite similar, a major difference of K–hypoplasticity as compared to CLoE stems from including void ratio in the set of state variables for the material through the pyknotropy factor f_d [13]. This allows the critical state concept to be incorporated in the model response.

The K–hypoplastic model provided by (6) can predict the behavior of fine-grained soils upon monotonic loading at medium to large strain levels. An enhanced version has been also proposed in [18] to improve the model performance in the small-strain range and for cyclic loading conditions. The constitutive equation for the enhanced model reads:

$$\dot{\boldsymbol{\sigma}} = \boldsymbol{\mathcal{M}}\,(\boldsymbol{\sigma}, e, \boldsymbol{\delta}, \boldsymbol{\eta}) : \dot{\boldsymbol{\epsilon}}, \tag{7}$$

where $\boldsymbol{\mathcal{M}}$ is the fourth-order tangent stiffness tensor of the material, $\boldsymbol{\eta} := \dot{\boldsymbol{\epsilon}}/\,\|\dot{\boldsymbol{\epsilon}}\|$ denotes the strain rate direction, and the additional state variable $\boldsymbol{\delta}$ is a symmetric second-order tensor called *intergranular strain* [23].

Let $\rho := \|\boldsymbol{\delta}\| / R$ be a suitable normalized magnitude of $\boldsymbol{\delta}$, R being a scalar model parameter, and

$$\hat{\boldsymbol{\delta}} = \begin{cases} \boldsymbol{\delta}/\|\boldsymbol{\delta}\| & \text{for } \boldsymbol{\delta} \neq \mathbf{0} \\ \mathbf{0} & \text{for } \boldsymbol{\delta} = \mathbf{0} \end{cases} \tag{8}$$

denote intergranular strain direction. The fourth-order tangent stiffness tensor $\boldsymbol{\mathcal{M}}$ is calculated from the constitutive tensors tensors $\boldsymbol{\mathcal{L}}$ and $\boldsymbol{\mathcal{N}}$ defined in (6) and the intergranular strain direction $\hat{\boldsymbol{\delta}}$ via the following interpolation:

$$\boldsymbol{\mathcal{M}} = [\rho^{\chi} m_T + (1 - \rho^{\chi}) m_R] f_s \boldsymbol{\mathcal{L}} + \boldsymbol{\mathcal{B}}, \tag{9}$$

where:

$$\boldsymbol{\mathcal{B}} := \begin{cases} \rho^{\chi}(1 - m_T) f_s \boldsymbol{\mathcal{L}} : \hat{\boldsymbol{\delta}} \otimes \hat{\boldsymbol{\delta}} + \rho^{\chi} f_s f_d \boldsymbol{\mathcal{N}} \otimes \hat{\boldsymbol{\delta}} & (\hat{\boldsymbol{\delta}} : \dot{\boldsymbol{\epsilon}} > 0). \\ \rho^{\chi}(m_R - m_T) f_s \boldsymbol{\mathcal{L}} : \hat{\boldsymbol{\delta}} \otimes \hat{\boldsymbol{\delta}} & (\hat{\boldsymbol{\delta}} : \dot{\boldsymbol{\epsilon}} \leq 0) \end{cases} \tag{10}$$

The evolution equation for the intergranular strain tensor $\boldsymbol{\delta}$ is given by

$$\dot{\boldsymbol{\delta}} = \begin{cases} \left(\boldsymbol{\mathcal{I}} - \hat{\boldsymbol{\delta}} \otimes \hat{\boldsymbol{\delta}} \rho^{\beta_r} \right) : \dot{\boldsymbol{\epsilon}} & (\hat{\boldsymbol{\delta}} : \dot{\boldsymbol{\epsilon}} > 0) \\ \dot{\boldsymbol{\epsilon}} & (\hat{\boldsymbol{\delta}} : \dot{\boldsymbol{\epsilon}} \leq 0) \end{cases} . \tag{11}$$

In (9)–(11), χ, m_T, m_R, and β_r are material constants. Full details of the mathematical structure of the model are provided in [18].

3.4 Calibration of the Models

When comparing the performance of different constitutive models in predicting the observed directional response of the material, a particular care must be taken in the proper selection of the procedure adopted for their calibration. In the present case, this task is somewhat facilitated by the fact that all the constitutive models considered, with the only exception of the CLoE hypoplastic model, incorporate the basic principles of critical state soil mechanics, and thus some of the material constants share the same physical meaning.

In order to separate the data used for the calibration of the different models and the data used for the evaluation of their performance, the material constants of the five models have been determined from the results of the stress probes starting from the isotropic initial state A. This is also consistent with the procedure typically used in practical applications, where most of the experimental data provided by the site investigation refer to isotropically consolidated, drained, or undrained triaxial tests.

For some of the constitutive models considered, the available data from stress probes at point A do not provide enough information to calibrate all the relevant constants. This is the case, for example, of the material parameters controling the response of the 3-SKH model and the enhanced K–hypoplastic model in the very small strain range. In such cases, the choice has been made to evaluate such material constants based on the experience gathered in previous

experimental investigations on similar soils. Although such a choice necessarily introduces a certain degree of subjectivity in the comparative evaluation of the models response, it can still be considered acceptable to our purposes, considering that the typical range of variation of such parameters for different soils is relatively limited, and the model response is not very sensitive to their variation, see e.g., [6, 23].

The calibration procedures are fully detailed in [20]. The resulting sets of material constants adopted for each model are reported in Tables 2 and 3. For the meaning of each constant and the initial values of the state variables adopted in the simulations, the reader is referred to [20].

Table 2. Material constants adopted for MCC, 3-SKH and K–hypoplastic models

material constant	MCC	3-SKH	K–hypo (standard)	K–hypo (enhanced)
N	2.245	–	–	–
λ	0.097	–	–	–
κ	0.017	–	–	–
M	1.33	1.33	–	–
G (MPa)	5.0	–	–	–
N^*	–	0.85	0.85	0.85
λ^*	–	0.057	0.057	0.057
κ^*	–	0.004	0.007	0.007
A	–	653.0	–	–
n	–	0.71	–	–
m	–	0.27	–	–
T	–	0.24	–	–
S	–	0.16	–	–
ψ	–	1.0	–	–
ϕ_c (deg)	–	–	33.0	33.0
r	–	–	0.4	0.4
m_R	–	–	–	3.5
m_T	–	–	–	3.5
R	–	–	–	10^{-4}
β_r	–	–	–	0.2
χ	–	–	–	6.0

Table 3. Material constants adopted for CLoE model

φ_c (deg.)	c (kPa)	χ_{ca} (–)	y_{ca} (–)	y_{rc} (–)	p_{fc} (–)	p_{ref} (kPa)	$\epsilon_{v,\mathrm{ref}}$ (–)	λ_c (–)	φ_e (deg.)
34.0	0	0.17	0.055	3.1	0	147.26	0.0	183.34	33
χ_d (–)	χ_c (–)	χ_{m2} (–)	y_e (–)	p_{fe} (–)	m_c (–)	m_e (–)	n (–)	ω (–)	
−1.0	−0.1	−0.05	0.011	0.02	−0.2	0.0	−0.2	0.36	

4 Observed vs. Predicted Response

In the following, the response of reconstituted Beaucaire Marl to the stress probing program detailed in Table 1 and the predictions of the different models described in Sect. 3 are depicted using the so-called *incremental strain response envelope*, as defined in [33]. Such a representation directly follows from the concept of response envelope – first proposed in [12] – by replacing stress and strain rates with finite-size stress and strain increments. In the general case, an incremental strain response envelope (RE, hereafter) is a "surface" in a six-dimensional space. However, for the particular loading conditions considered, the most natural choice is to represent the section of the REs in the plane of work-conjugated strain increment quantities, $(\Delta\epsilon_a, \sqrt{2}\,\Delta\epsilon_r)$, see Fig. 1b. The size of each strain increment vector defining the RE can be directly interpreted as a directional secant compliance of the material, for the associated loading direction and stress increment magnitude.

Figures 4 and 5 show the computed REs for all the model considered at small to medium stress increment levels ($R_\sigma = 20$, 30, 40, and 50 kPa), and at medium to large stress increment levels ($R_\sigma = 50$ and 90 kPa), respectively. The corresponding experimental REs are also shown on the top left corner of both figures.

For small to medium stress increment levels, the experimental REs indicate that the softest response is associated to those paths which are characterized by a large deviatoric component (e.g., tests Tx119 and Tx113). As R_σ increases, the envelopes progressively shift upward to the left, due to the fact that the initial state is closer to the critical state line for axisymmetric compression than to the corresponding line for axisymmetric extension. For $\eta = 0.4$ loading paths (Tx130 and Tx129), the material response is softer when the probe points in the direction of continued loading, and stiffer upon unloading (i.e., upon full stress path reversal with respect to the consolidation history). In fact, this last path corresponds to the stiffest response of the material. A direct consequence of the above observations is that the experimental REs are markedly nonsymmetric about the origin of the strain increment space.

The predictions of the different models considered appear, from a qualitative standpoint, all in fair agreement with the salient features of the experimental response discussed earlier. The only notable exception is represented by the predictions of CLoE model upon $\eta = 0.4$ loading paths, where – contrary to experimental evidence – no significant difference between secant stiffnesses in compression and extension is observed. From a quantitative standpoint, however, all models appear to significantly underpredict the secant stiffness of the material. The REs predicted by the two elastoplastic models have a convex shape, except for the expected, yet minor irregularity of the Modified Cam-Clay envelopes, close to neutral loading in extension. The REs of the two K–hypoplastic models, and (to a much lesser extent) those of CLoE show

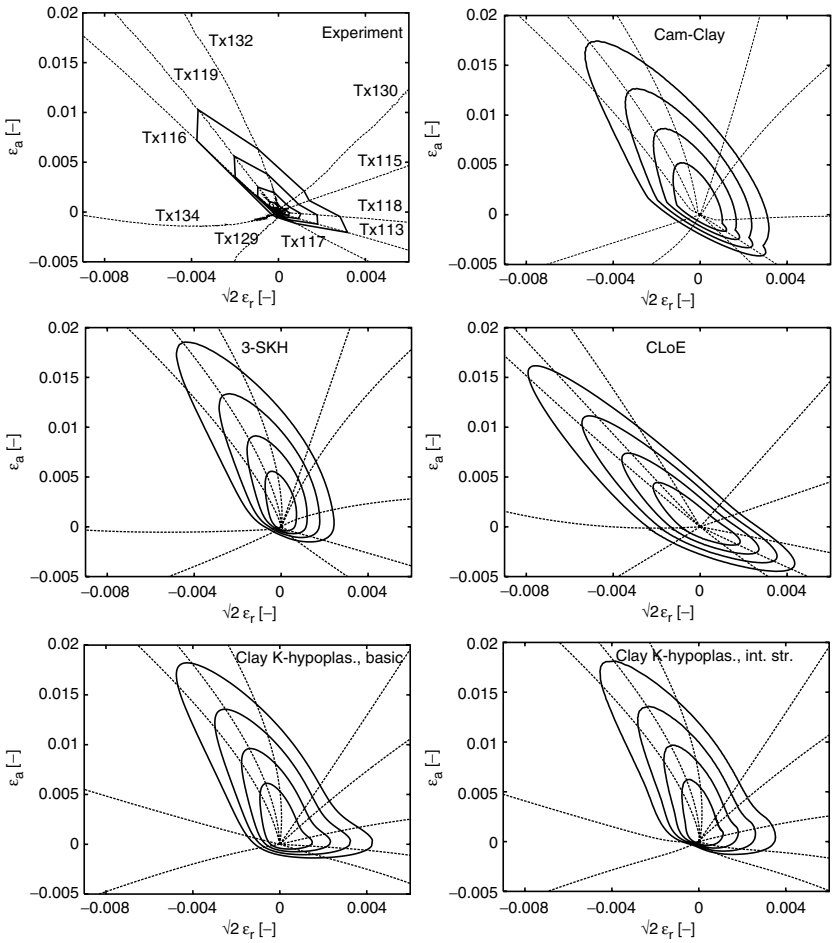

Fig. 4. Experimental vs. simulated strain response envelopes for $R_\sigma = 20$, 30, 40, and 50 kPa

some degree of nonconvexity in a region located around the $\eta = 0.4$ loading direction. This feature is also shown by the two largest experimental REs, although such an observation is based on the results of one single stress-probe.

At large stress increment level ($R_\sigma = 90$ kPa, Fig. 5), both the elastoplastic and the K–hypoplastic models provide response envelopes which appear in fairly good agreement with the experimental results, both from a qualitative and a quantitative point of view. On the contrary, CLoE significantly underestimates soil stiffness for loading paths close to deviatoric compression (Tx116 and Tx119).

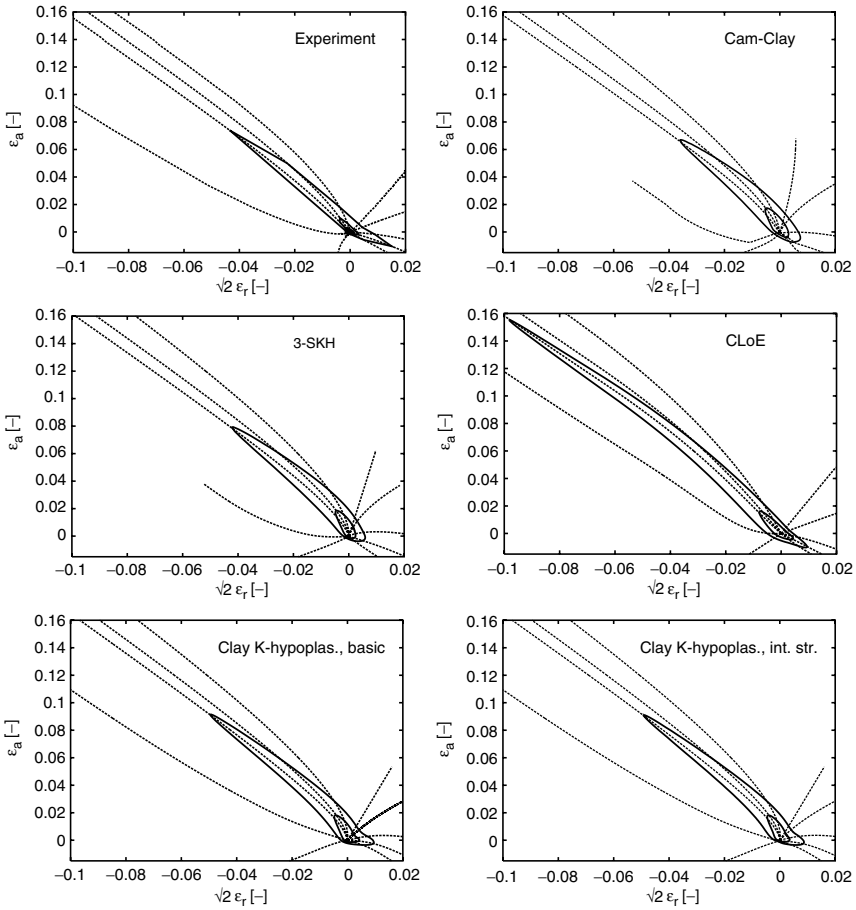

Fig. 5. Experimental vs. simulated strain response envelopes for $R_\sigma = 50$ and 90 kPa

5 Concluding Remarks

The comparative evaluation of the performance of different constitutive models in their application to the quantitative solution of practical engineering problems is a very complex task, which typically requires the consideration of a number of key issues, such as: the capability of reproducing the relevant experimental response; the relative complexity of the calibration procedures; the number and nature of the internal state variables describing the effects of previous loading history; the availability of robust and accurate algorithms for their numerical implementation in FE codes, etc. In this paper, the attention is focused on the qualitative and quantitative agreement between experimentally observed response and model predictions at the element level.

In standard practice, the comparison between model predictions and experimental results is typically done with reference to a limited number of conventional stress paths, whereas the response of the material for different loading conditions is extrapolated in a more or less reasonable way. This can be quite sufficient to assess the model performance in practical applications, whenever the problem at hand is such that most of the soil affected by the imposed loading conditions undergoes very similar stress paths, and one of such paths is included among those explored in the laboratory testing program. Unfortunately, this is only seldom the case in many important applications where an accurate prediction of soil–structure interaction processes and of the displacement field around the structure is required. Notable examples in this respect are provided by deep excavations and shallow tunnels to be realized in urban environments, as in such cases, different zones of soil experience widely different stress-paths, both in size and direction, and the quality of numerical predictions crucially relies on the ability of the constitutive model adopted for the soil to accurately reproduce the material response along all such loading paths.

In this paper, an attempt is made to evaluate the response of different advanced constitutive models for fine-grained soils in more general terms, considering their predictive capabilities over a quite wide range of loading conditions. While the strain response envelopes plotted in Figs. 4 and 5 provide a clear qualitative picture of the performance of the five models considered, a more quantitative comparison of model predictions has been presented in [20] by introducing a suitable scalar measure of the "distance" between model responses and experimental results. Based on such a comparison, the best performance overall appears to be provided by the enhanced K–hypoplastic model and the 3-SKH model, at both small and large strain levels.

As compared to its enhanced version, the performance of the standard K–hypoplastic model is still reasonably good, mainly because the loading programs considered involve only a very limited number of stress reversals. For the application to monotonic (or quasimonotonic) loading conditions, the standard K–hypoplastic model may therefore represent a valid alternative to more complex formulations. On the contrary, the performance of CLoE model appears quite poor as compared to the other elastoplastic or hypoplastic models, particularly for those loading paths involving a significant increase in mean stress. This is not surprising, considering that CLoE is a first-generation hypoplastic model, in which the stress tensor is the only state parameter. For this reason, the mathematical structure of CLoE does not allow to properly distinguish normally consolidated and overconsolidated states, and to correctly describe critical state failure conditions. While CLoE has demonstrated its capability of accurately modeling the response of coarse-grained soils along mainly deviatoric loading paths, see e.g., [5], these limitations obviously make it unfit to model the behavior of soft clays. An attempt to modify the current version of CLoE in order to improve its performance for normally consolidated clays has been recently presented by [19].

It is worth noting that even the predictions of the classical Cam-Clay model for those paths which point outside the initial yield surface are quite good, and essentially equivalent to those obtained with 3-SKH model. This is to be expected, as the soil considered in this study was in a (almost) normally consolidated state.

Both the enhanced K–hypoplastic model and the 3-SKH model are characterized by a relatively limited number of constants, most of which are linked to standard features of clay behavior. In fact, all the constants appearing in these two models can be determined by means of standard laboratory tests, with the only exception of those controling the stiffness of the material at very low strain levels. Of course, the above considerations also apply to the simpler standard K–hypoplastic model for clays, which possesses only five constants, just like the classical Modified Cam-Clay. On the other hand, CLoE model requires a much wider pool of experimental data to determine the relatively large number of constants. Moreover, as CLoE constants typically control more than one specific feature of the material response, they cannot be determined independently. Rather, they have to be found by means of a complex calibration procedure which has to be implemented numerically in a suitable calibration code. This represents a second, major drawback of the CLoE model as compared to the more recent K–hypoplastic models for clays.

Acknowledgment

The second author is grateful for the financial support by the research grants SSPI-CT-2003–501837-NOAH'S ARK under the EC 6th FP and GACR 205/03/1467.

References

1. A. Al Tabbaa and D.M. Wood. An experimentally based "bubble" model for clay. In *Proceeding of 3rd International Conference on Numerical Models in Geomechanics*. Niagara Falls, 1989
2. J.H. Atkinson, D. Richardson, and S.E. Stallebrass. Effects of recent stress history on the stiffness of over–consolidated soil. *Géotechnique*, 40(4):531–540, 1990
3. L. Callisto and G. Calabresi. Mechanical behaviour of a natural soft clay. *Géotechnique*, 48(4):495–513, 1998
4. R. Chambon and J. Desrues. Bifurcation par localisation et non linéarité incrémentale: un example heuristique d'analyse complete. In *Plastic Instability*, pages 101–113, Paris, France, 1985. Presses ENPC
5. R. Chambon, J. Desrues, W. Hammad, and R. Charlier. CLoE, a new rate–type constitutive model for geomaterials. theoretical basis and implementation. *Int. J. Numer. Anal. Methods Geomech.*, 18:253–278, 1994
6. C.R.I. Clayton and G. Heymann. Stiffness of geomaterials at very small strains. *Géotechnique*, 51(3):245–255, 2001

7. D. Costanzo, G. Viggiani, and C. Tamagnini. Directional response of a reconstituted fine–grained soil. Part I: experimental investigation. Int. J. Num. Anal. Meth. Geomech. (in print), 2006
8. F. Darve. The expression of rheological laws in incremental form and the main classes of constitutive equations. In F. Darve, editor, *Geomaterials: Constitutive Equations and Modelling*, pages 123–148. Elsevier, Amsterdam, 1990
9. J. Desrues and R. Chambon. Shear band analysis for granular materials: the question of incremental non–linearity. *Ingenieur–Archiv*, 59:187–196, 1989
10. R.J. Finno, I.S. Harahap, and P.J. Sabatini. Analysis of braced excavations with coupled finite element formulations. *Comput. Geotech.* 12:91–114, 1989
11. J. Graham, M.L. Noonan, and K.V. Lew. Yield states and stress-strain relationships in natural plastic clay. *Can. Geotech. J.*, 20:502–516, 1983
12. G. Gudehus. A comparison of some constitutive laws for soils under radially symmetric loading and unloading. In Wittke, editor, *3rd Int. Conf. Numer. Methods Geomech.*, Aachen, pages 1309–1324. Balkema, Rotterdam, 1979
13. G. Gudehus. A comprehensive constitutive equation for granular materials. *Soils Found.* 36(1):1–12, 1996
14. K. Hashiguchi. Two– and three–surface models of plasticity. In *V International Conferance of Numerical Methods in Geomechanics*, pages 285–292, Nagoya, Japan, 1985. Balkema, Rotterdam
15. D. Kolymbas. An outline of hypoplasticity. *Arch. Appl. Mech.* 61:143–151, 1991
16. J. Lanier, D. Caillerie, R. Chambon, and G. Viggiani. A general formulation of hypoplasticity. *Int. J. Numer. Anal. Methods Geomech.*, 28:1461–1478, 2004
17. P.I. Lewin and J.B. Burland. Stress-probe experiments on saturated normally consolidated clay. *Géotechnique*, 20(1):38–56, 1970
18. D. Mašín. A hypoplastic constitutive model for clays. *Int. J. Numer. Anal. Methods Geomech.*, 29:311–336, 2005
19. D. Mašín, R. Chambon, and J. Desrues. CLoE model modified to predict the behaviour of normally compressed clays. In *Proc. 11th Int. Conf. IACMAG*. Turin, Italy, 2005
20. D. Mašin, C. Tamagnini, D. Costanzo, and G. Viggiani. Directional response of a reconstituted fine–grained soil. Part II: performance of different constitutive models. Int. J. Num. Anal. Meth. Geomech., (in print), 2006
21. Z. Mroz, V.A. Norris, and O.C. Zienkiewicz. An anisotropic hardening model for soils and its application to cyclic loading. *Int. J. Numer. Anal. Methods Geomech.*, 2:203–221, 1978
22. A. Niemunis. *Extended Hypoplastic Models for Soils*. Habilitation thesis, Ruhr-University, Bochum, 2002
23. A. Niemunis and I. Herle. Hypoplastic model for cohesionless soils with elastic strain range. *Mech. Cohesive–Frictional Mater.* 2:279–299, 1997
24. J.H. Prevost. Mathematical modelling of monotonic and cyclic undrained clay behaviour. *Int. J. Numer. Anal. Methods Geomech.*, 1:195–216, 1977
25. J.R. Rice. The localization of plastic deformations. In Koiter, editor, *Theoretical and Applied Mechanics*, pages 207–220. North–Holland, 1976
26. K.H. Roscoe and J.B. Burland. On the generalised stress-strain behaviour of wet clay. In J. Heyman and F.A. Leckie, editors, *Engineering Plasticity*, pages 535–609. Cambridge University Press, Cambridge, 1968
27. J.W. Rudnicki and J.R. Rice. Conditions for the localization of deformation in pressure–sensitive dilatant materials. *J. Mech. Phys. Solids*, 23:371–394, 1975

28. P.R. Smith, R.J. Jardine, and D.W. Hight. The yielding of Bothkennar clay. *Géotechnique*, 42(2):257–274, 1992
29. H.D. St. John, D.M. Potts, R.J. Jardine, and K.G. Higgins. Prediction and performance of ground response due to construction of a deep basement at 60 Victoria Embankment. In G.T. Houlsby and A.N. Schofield, editors, *Predictive Soil Mechanics (Wroth Mem. Symp.)*. Thomas Telford, London, 1993
30. S.E. Stallebrass. *Modelling the effect of recent stress history on the behaviour of overconsolidated soils*. PhD thesis, The City University, London, 1990
31. S.E. Stallebrass and R.N. Taylor. Prediction of ground movements in overconsolidated clay. *Géotechnique*, 47(2):235–253, 1997
32. C. Tamagnini and G. Viggiani. On the incremental non-linearity of soils. Part I: theoretical aspects. *Rivista Italiana di Geotecnica*, 36(1):44–61, 2002
33. C. Tamagnini, G. Viggiani, R. Chambon, and J. Desrues. Evaluation of different strategies for the integration of hypoplastic constitutive equations: Application to the CLoE model. *Mech. Cohesive–Frictional Mater.* 5:263–289, 2002
34. C.A. Truesdell. Hypo–elastic shear. *J. Appl. Phys.* 27:441–447, 1956
35. G. Viggiani and C. Tamagnini. Ground movements around excavations in granular soils: a few remarks on the influence of the constitutive assumptions on FE predictions. *Mech. Cohesive–Frictional Mater.* 5(5):399–423, 2000
36. A.J. Whittle, Y.M.A. Hashash, and R.V. Whitman. Analysis of deep excavation in Boston. *J. Geotech. Engng. ASCE*, 119(1):69–90, 1993
37. D.M. Wood. *Some aspects of the mechanical behavior of Kaolin under truly triaxial conditions of stress and strain*. PhD thesis, Cambridge University, Cambridge, 1974
38. W. Wu and D. Kolymbas. Hypoplasticity then and now. In D. Kolymbas, editor, *Constitutive Modelling of Granular Materials*. Springer, Berlin Heidelberg New York, 2000